Precision Agriculture (2023) 24:607–626
https://doi.org/10.1007/s11119-022-09961-9

Spectral reflection and crop parameters: can the disentanglement of primary and secondary traits lead to more robust and extensible prediction models?

Maren Rose[1] · **Till Rose**[1] · **Henning Kage**[1]

Accepted: 28 September 2022 / Published online: 8 October 2022

Abstract

Recently the application of spectral reflection data for the prediction of crop parameters for applications in precision agriculture, such as green area index (GAI), total aboveground dry matter (DM), and total aboveground nitrogen content (N content) increases. However, the usability of vegetation indices (VI) for the prediction of crop parameters is strongly limited by the fact that most VI calibrations are only valid for specific crops and growth periods. The results of the presented study based on the differentiation of primary (main driver of the reflectance signal) and secondary (not directly related to reflectance signal) crop parameters. For GAI prediction, a universal (without crop-specific parametrization) simple ratio vegetation index (SR) provided good calibration (R^2 adj. = 0.90, MAE = 0.32, rMAE = 22%) and evaluation results (MAE = 0.33, rMAE = 18%). The disentanglement of primary and secondary traits allowed the development of a functional two-step model for the estimation of the N content during vegetative growth (MAE = 19.2 g N m^{-1}, rMAE = 44%). This model was based on fundamental, crop-specific relationships between the crop parameters GAI and N content. Additionally, an advanced functional approach was tested enabling the whole-season prediction of DM and confirming a reliable GAI estimation throughout the whole growing season (R^2 = 0.89–0.93).

Keywords Green area index · Total aboveground dry matter · Nitrogen content · Simple ratio vegetation index · Functional two-step model

Introduction

Key traits for the purpose of precision farming, yield estimation, global carbon cycling or the calibration and application of crop growth models, such as green area index (green plant area per ground area; GAI), leaf area index (LAI), total aboveground dry matter (DM), and total aboveground nitrogen content (N content) are often required in a high spatial and temporal resolution. These traits are derivable from spectral

✉ Maren Rose
radke@pflanzenbau.uni-kiel.de

[1] Institute of Crop Science and Plant Breeding, Agronomy and Crop Science Group, Christian-Albrechts-University, Hermann-Rodewald-Str. 9, 24118 Kiel, Germany

reflectance measurements which are detectable by several carrier systems, such as satellites, unmanned aerial vehicles (UAVs) and handheld devices (Bukowiecki et al., 2021; Gerighausen et al., 2015; Hansen & Schjoerring, 2003; Müller et al., 2008; Rosso et al., 2022). In general, the advantageous features of spectral remote sensing are speed, non-destructivity, and scalability. Hence, over the last decades, the application of spectral reflectance data for the prediction of various crop parameters in the agricultural context increased continuously (Fu et al., 2021; Weiss et al., 2020).

The spectral reflectance signal of a crop is primarily determined by the specific properties of its green parts and the probability that a light quantum hits either the crop or the soil surface (Christensen & Goudriaan, 1993; Gitelson et al., 2003; Tucker et al., 1981). Therefore, Weiss et al. (2020) proposed the classification of crop parameters in primary and secondary traits, whereby primary traits are involved in the process of radiative transfer, and hence, are directly derivable from spectral reflectance measurements. GAI is a key influential factor of these primary traits (Weiss et al., 2020). This is reflected in the existence of vegetation indices (VIs) for the estimation of GAI which are applicable throughout the whole growing season (Bukowiecki et al., 2020) and do not require a crop-specific parametrization (Delegido et al., 2013; Dong et al., 2020; Kira et al., 2016; Nguy-Robertson et al., 2012; Viña et al., 2011). From this, the first working hypothesis of the presented study was deduced:

1. GAI is the major determinant of spectral reflectance. Therefore, VIs for the GAI estimation can be calibrated uniformly for a range of crops and applied throughout their whole growing season.

In contrast, the estimation of secondary variables (e.g., N content or DM) must contain crop-specific factors as the relationship between GAI and these traits varies between crops (Lemaire et al., 2008). Nevertheless, such crop parameters play an important role in the application of some agronomic traits. For example, a spatial and temporal knowledge of the crop nitrogen (N) status is highly relevant for an accurate site-specific fertilizer management. Thus, research forges ahead to find new options to derive information about secondary crop parameters from spectral reflectance data. A well working but very time-consuming and labor-intensive option is to fit daily calibrations (Ma et al., 2019). An alternative method is to couple simple crop growth models with the primary trait GAI and to deduce secondary traits as state variables (Claverie et al., 2012; Dong et al., 2020; Fu et al., 2021; Gerighausen et al., 2015; Weiss et al., 2020).

Recently, Lemaire et al. (2021) argued for the usage of spectral reflectance data in the agricultural context by a coherent theoretical framework which should be based on existing fundamental relationships to apply this technology in a useful and robust way. Those fundamental relationships often can be found between the secondary traits N content as well as DM and the primary trait GAI. However, these correlations are always crop-specific, restricted to the vegetative growth period and affected by several other factors, such as N treatment, environment, and water status (e.g., Lemaire et al., 2007; Muchow & Sinclair, 1994; Vos et al., 2005). This led to the second working hypothesis of the presented study:

2. The disentanglement of the spectral reflection signal and secondary traits by the consideration of existing fundamental relationships provides the development of more robust prediction models for the estimation of secondary variables, such as DM and N content.

Robust and easily extensible models for the prediction of the crucial crop parameters GAI, DM, and N content by the measurement of spectral reflectance might be achieved more reliable by the combination of both working hypotheses because confounding variables as well as differing growth periods might be detected more directly. Additionally, the combination of a universal GAI model and fundamental relationships between primary and secondary traits would permit the usage of larger and incomplete datasets.

To test the working hypotheses, a large unpublished dataset was analyzed. Data were collected in the last two decades and comprised four crops (winter oilseed rape, winter wheat, winter barley, and silage maize) and different N treatments ranging from no fertilization to substantial oversupply.

Materials and methods

Study site and field trials

Data were collected between 2003 and 2020 in several field trials containing different crops (winter wheat, winter barley, winter oilseed rape, and silage maize) and N treatments. All field trials were carried out in Northern Germany at the Hohenschulen Experimental Farm of the Kiel University (10.0 E, 54.3 N, 30 m a.s.l.). The study site is characterized by Luvisol soils with sandy loam textures in the topsoil (Food and Agriculture Organization of the United Nations, 2014). The long-term mean annual temperature is about 8.8 °C, the annual precipitation averages 806 mm, thereof 462 mm occurs during main growing season between March and September.

Data collection

Datasets

This study is based upon three datasets described in more detail below (Fig. 1; Table 1). All datasets contained different N treatments ranging from no fertilization to substantial oversupply and different crops. Dataset I and Dataset II provide data for the calibration and evaluation of the prediction models during vegetative growth for the target crop parameters GAI, DM, and N content. Dataset III comprise data collected during the whole growing season and was used for the development of an advanced functional model for whole-season DM prediction (Fig. 1).

Dataset I consists of 1482 samples in total collected in nine field trials between 2005 and 2018. It was split in two subsets: Calibration Set and Evaluation Set (Fig. 1; Table 1). To create two independent datasets, measurements collected on a certain sampling date were either assigned to the Calibration Set or to the Evaluation Set. Thus, erroneous overfitting due to date-specific measurement errors was adequately penalized in the evaluation. The Calibration Set comprises two crops (winter wheat and winter oilseed rape) and GAI ranged from 0 to 6.7, DM ranged from 0.8 to 685 g DM m^{-2}, and N content ranged from 0.03 to 20.3 g N m^{-2}. The independent Evaluation Set contains four crops (winter wheat, winter oilseed rape, silage maize, and winter barley) and includes GAI values ranging from 0.03 to 7.7, DM values ranging from 0.3 to 809 g m^{-2}, and N contents values ranging from 0.02 to 20.4 g N m^{-2}. Data for both sets were collected during vegetative growth between BBCH main stage 1 (leaf development) and the end of BBCH main stage 5 (inflorescence

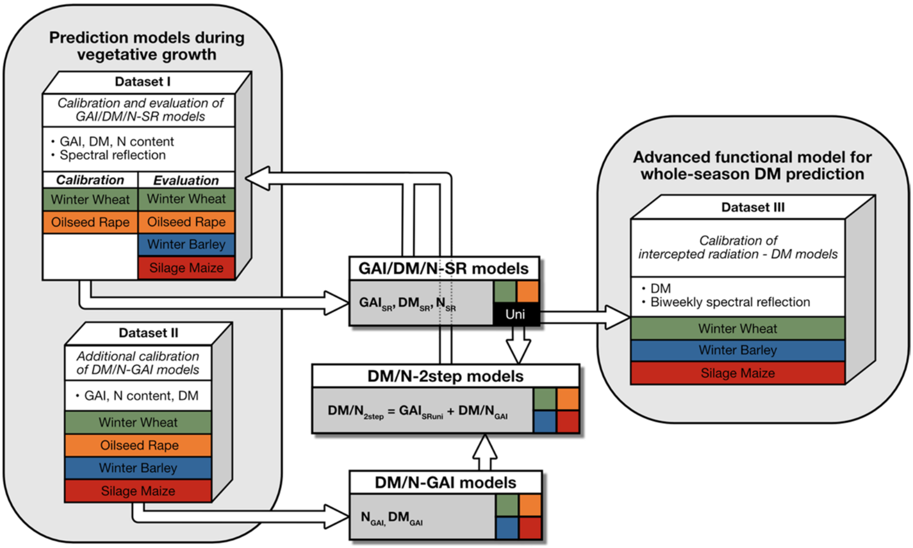

Fig. 1 Flowchart of the considered datasets and the main processes of the data analysis

Table 1 Overview of the data comprised in Dataset I, Dataset II, and Dataset III (n represents the number of collected data)

Dataset	Crop	GAI (n)	DM [g m^{-2}] (n)	N content [g m^{-2}] (n)
Dataset I (Calibration Set)	Winter Oilseed Rape	0.02–3.2 (231)	0.8–537 (231)	0.03–20.1 (231)
	Winter Wheat	0–6.7 (206)	31–685 (126)	1.1–20.3 (126)
Dataset I (Evaluation Set)	Winter Oilseed Rape	0.02–2.7 (192)	1–284 (215)	0.05–13.1 (119)
	Silage Maize	0.03–5 (154)	0.3–669 (235)	0.01–17.3 (235)
	Winter Barley	0.1–5.8 (164)	17–809 (198)	0.3–17.8 (198)
	Winter Wheat	0.4–7.7 (329)	15–788 (119)	0.6–20.4 (119)
Dataset II	Winter Oilseed Rape	0.01–4.5 (530)	1–485 (530)	0.09–21.9 (530)
	Silage Maize	0.04–6.4 (123)	1–707 (123)	0.06–19.8 (123)
	Winter Barley	0.07–4.4 (95)	7–625 (95)	0.3–10.6 (95)
	Winter Wheat	0.01–6.5 (696)	0.3–929 (696)	0.01–20.3 (696)
Dataset III	Silage Maize		35–1925 (157)	
	Winter Barley		24–1705 (65)	
	Winter Wheat		15–2053 (216)	

GAI green area index, *DM* total aboveground dry matter, *N content* total aboveground nitrogen content

emergence). For each data point, spectral reflection measurements in parallel with destructive plant samplings were available. Not every crop parameter was captured at each sampling date, thus, the number of data points vary for the different calibration and evaluation purposes (Table 1).

Dataset II consists of 2224 data points collected in twelve field trials between 2003 and 2020 (Table 1). It includes the crops winter wheat, winter barley, winter oilseed rape, and silage maize. Samples were harvested during vegetative growth between BBCH main stage 1 (leaf development) and the end of BBCH main stage 3 (stem elongation) for winter wheat, winter barley, and silage maize or the end of BBCH main stage 5 (inflorescence emergence) for winter oilseed rape, respectively. GAI, DM, and N content were destructively determined for each sample.

Dataset III consists of measurements and samplings collected in a crop rotation field trial between 2016 and 2018 (Table 1). Spectral reflectance data were collected for winter wheat, winter barley, and silage maize weekly to biweekly between March and harvest. Destructive DM samples were collected in several plots throughout the growing season. Plots were harvested by combine and additionally by hand.

Plant samplings

In two experiments of the Evaluation Set (Dataset I) GAI data were captured non-destructively using a plant canopy analyzer (LAI-2000 or LAI-2200, LiCor Inc., NE, USA). Apart from that, GAI, DM, and N concentration were determined by destructive sampling of the aboveground plant material of a defined and representative area of the plot (0.25 m^2 for winter wheat and winter barley, 1 m^2 for winter oilseed rape, 10 plants for silage maize). After determining the developmental stage by the BBCH-scale (Meier, 1997) the samples were further processed. Collected plants were separated in green leaves, green stems, and senescent parts of the plant. The green leaf area index and green stem area index were determined using a LI-3100 leaf area meter (LiCor Inc., NE, USA), and GAI was calculated as their sum. Subsequently, the samples were dried, weighted, ground and the N concentration was analyzed by near infrared spectroscopy (NIRS; NIRSystems 5000 scanning monochromator, FOSS GmbH, Rellingen, Germany). Therefore, the N concentration of a calibration and an evaluation dataset was determined using a Vario Max CN analyzer (Elementar Analysensyteme, Hanau, Germany). The N content of the aboveground biomass was calculated by multiplying the total aboveground dry matter and the determined N concentration.

Spectral reflectance measurements

Hyperspectral reflectance measurements were carried out with a HandySpec® Field spectrometer (tec5 AG, Oberursel, Germany), a handheld device with an opening angle of 25° that is hold about 1 m above the crop and measures in 10 nm steps between 400 and 1000 nm. At the beginning of each sampling date, the optical sensors of the spectrometer were technically calibrated with a white standard. Due to noise at the end of the measured spectrum, only data between 400 and 900 nm were used for further analyses. In total, three to five measurements per sampling plot were averaged to represent the reflectance spectrum of the whole plot. In Dataset I, the hyperspectral reflectance measurements were carried out directly before destructive sampling at the defined sampling area of the plot. The measurements in Dataset III were distributed over the entire plot (plot size: 3×7 m).

Data processing and statistical analysis

Data processing and statistical analyses were conducted in the statistical environment R (R Core Team, 2000). For visualization, the package ggplot2 was used (Wickham, 2016).

In Fig. 1, the main processes of calibration, evaluation, and application were illustrated to clarify the procedure of the data analysis.

Model calibration and evaluation of simple ratio vegetation indices for the target crop parameters

It is common practice to convert the spectral reflectance at two or more wavelengths into VIs which can be formulated in different ways (e.g., Bukowiecki et al., 2020; Christensen & Goudriaan, 1993; Clevers & Kooistra, 2012; Demetriades-Shah et al., 1990). Simple ratio vegetation indices (SRs), initially published by Jordan (1969), divide the reflectance in one wavelength by another. Since SRs are easily-to-handle, they are frequently used. SRs have been shown to be sensitive and linear correlated to several crop parameters (Bukowiecki et al., 2020; Clevers & Gitelson, 2013; Serrano et al., 2000; Viña et al., 2011).

The entire Calibration Set (Dataset I) was analyzed to calibrate universal (without crop-specific parametrization) SRs for the target crop parameters GAI (GAI_{SRuni}), DM (DM_{SRuni}), and N content (N_{SRuni}). Additionally, the Calibration Set was split in the individual crops. Hence, the calibration of crop-specific SRs for winter wheat to estimate GAI (GAI_{SRww}), DM (DM_{SRww}), and N content (N_{SRww}), and for winter oilseed rape to estimate GAI (GAI_{SRwosr}), DM (DM_{SRwosr}), and N content (N_{SRwosr}) was possible. Therefore, simple linear and quadratic regressions between the target crop parameters (GAI, DM, and N content) and all possible wavelength combinations ($n=2550$) were fitted. The superior models and the associated best wavelength combinations for the individual SRs were selected by comparing the adjusted correlation coefficient (R^2 adj.) of the linear and the quadratic equations.

The performance of the established SRs was evaluated in the independent Evaluation Set (Dataset I). The mean absolute error (MAE) and the relative MAE (rMAE) were used for the assessment of the applied models. To examine whether crop, N treatment, year, and the combination of these factors affected the models, the R^2 adj. for the simple linear regression, the linear regression with every additional factor, and the linear regression with all additional factors, and their interactions were calculated. The additionally explained variance was the difference between the base model and the extended models.

Calibration and evaluation of functional two-step models for secondary crop parameters

The functional two-step DM model (DM_{2step}) and a functional two-step N content model (N_{2step}) were developed assuming a strong but crop-specific correlation between GAI and DM or GAI and N content, respectively.

According to Lemaire et al. (2007), GAI and DM are allometrically related. This relation is described by a power function:

$$GAI = c \times DM^{a}, \tag{1}$$

where parameter c is the so-called "leafiness coefficient" and represents the GAI of the crop at $DM = 1$ t ha^{-1}. Parameter c depicts morphological differences and is crop-specific (Lemaire et al., 2007). Parameter a is the ratio between the relative rate of GAI expansion and the relative rate of DM accumulation.

In addition, a linear relationship between GAI and N content exists (Lemaire et al., 2007):

$$\text{N content} = \frac{b}{c} \times \text{GAI}. \tag{2}$$

Parameter b is the accumulated N content of the crop at DM = 1 t ha^{-1} and represents the ability of a crop to accumulate N during the early growth period. Parameter b differs between C3 and C4 crops due to metabolic differences, but it is rather constant for species within these groups (Lemaire et al., 2007). Parameter c is the "leafiness coefficient" described above.

In Dataset II the crop-specific relations between GAI, DM, and N content, and the crop-specific response to N deficiency were investigated. As stated by Lemaire et al. (2007), power functions between GAI and DM were calculated (Eq. 1). Linear and power functions were fitted between the crop parameters GAI and N content because non-linearity was apparent in the presented dataset. The superior models were selected by comparing the R^2 adj.

The evaluation of DM_{2step} and N_{2step} was conducted in the Evaluation Set (Dataset I). Therefore, GAI was predicted by GAI_{SRuni}, and the estimated values were multiplied with the detected crop-specific correlations between GAI and the secondary crop parameters. The assessment of the functional two-step models was carried out in the same way as for the SRs described above.

Development of an advanced functional model for DM prediction

An advanced functional model for DM prediction throughout the whole growing period was devised.

According to Monteith (1977), the generated DM is the product of intercepted radiation (Q) and radiation use efficiency (RUE). RUE is defined as ratio between Q and DM in a certain time interval:

$$\text{DM} = \text{RUE} \times \text{Q}. \tag{3}$$

GAI_{SRuni} was applied to the spectral reflectance measurements in Dataset III to predict GAI at every measuring date. The GAI development on plot level for a daily timestep was assigned by linear interpolation. Based on this data, the amount of the intercepted radiation (Q) can be described by Beer-Lambert law (Monsi & Saeki, 1953):

$$\text{Q} = \text{I}_{\text{PAR}} \times (1 - e^{-k \times \text{GAI}}), \tag{4}$$

where I_{PAR} is the incoming photosynthetically active radiation and k the extinction coefficient. I_{PAR} is defined as total global radiation multiplied by the factor 0.5 and was weighted by a crop-specific temperature weighting factor. Therefore, a trapezoidal function ranging between 0 and 1 was used. The transition points were at 2.5, 9.5, 20, and 35 °C of the daily mean temperature for winter wheat and winter barley, and at 6, 16, 28, and 34 °C of the daily mean temperature for silage maize. For winter wheat and winter barley k was fixed at 0.729, and for silage maize k was fixed at 0.654 (own unpublished measurements).

Results

Model calibration and evaluation of simple ratio vegetation indices for the target crop parameters

In most cases, a quadratic fit between the SRs and the crop parameter performed best (highest R^2 adj.), except for the crop-specific GAI and N content models of winter wheat (Table 2). In case of the secondary crop parameters DM and N content, the data of all crops of the Calibration Set except of winter oilseed rape, were restricted to samples collected before the end of BBCH main stage 3 (stem elongation). Because samples collected afterwards caused large scattering mainly due to underestimation (data not shown).

The R^2 adj. of the calibration of all tested GAI models (universal and crop-specific) ranged from 0.89 to 0.91. The MAEs were between 0.18 and 0.37, and the rMAEs were between 18 and 22% (Table 2). The MAEs and the rMAEs of the evaluation were low as well (Table 3; Fig. 2). GAI_{SRuni} provided adequate GAI estimations for each crop of the Evaluation Set (MAE = 0.22–0.42, rMAE = 16–24%) and the model was not improved by additional factors (Tables 3, 4). The slope (0.871) of the linear regression between measured and predicted values indicated a slight underestimation of high GAI values by GAI_{SRuni}. However, no obvious saturation effects occurred in the Evaluation Set (Fig. 2).

The calibration of crop-specific SRs for the estimation of the N content resulted in higher assessment variables compared to the universal SR (Table 2). The evaluation of N_{SRuni} was affected by crop, year, and N treatment resulting in little saturation effects and scattering (Fig. 2; Table 4).

The universal and crop-specific DM models achieved MAEs between 27.02 and 38.1 g m^{-2} and rMAEs between 16 and 28% in the calibration. The R^2 adj. ranged from

Table 2 Best wavelength combinations for the estimation of green area index (GAI), total aboveground dry matter (DM), and total aboveground nitrogen content (N content) by simple ratio vegetation indices (SR)

Crop parameter	SR	VI	Equation	R^2 adj.	MAE (rMAE)
GAI	R760/R740	GAI_{SRww}	$-10.79 + 10.36 \cdot SR$	0.91	0.37 (18%)
	R750/R730	GAI_{SRwosr}	$-2.71 + 0.315 \cdot SR + 2.284 \cdot SR^2$	0.89	0.18 (22%)
	R810/R710	GAI_{SRuni}	$-0.97 + 0.91 \cdot SR - 0.02 \cdot SR^2$	0.90	0.32 (22%)
N content [g m^{-2}]	R780/R740	N_{SRww}	$-30.68 + 29.57 \cdot SR$	0.93	0.94 (14%)
	R750/R730	N_{SRwosr}	$8.47–38.43 \cdot SR + 29.5 \cdot SR^2$	0.92	0.91 (21%)
	R720/R710	N_{SRuni}	$18.72–40.47 \cdot SR + 22.25 \cdot SR^2$	0.88	1.24 (24%)
DM [g m^{-2}]	R760/R750	DM_{SRww}	$-2747 + 1921 \cdot SR - 801 \cdot SR^2$	0.92	36.23 (16%)
	R770/R430	DM_{SRwosr}	$-41.6 + 17.1 \cdot SR + 0.12 \cdot SR^2$	0.85	27.02 (28%)
	R810/R670	DM_{SRuni}	$-15.1 + 23.02 \cdot SR - 0.26 \cdot SR^2$	0.87	38.10 (27%)

VI vegetation index; *R^2 adj.* adjusted correlation coefficient; *MAE* mean absolute error; *rMAE* relative MAE

GAI_{SRww} crop-specific SR for GAI prediction of winter wheat, GAI_{SRwosr} crop-specific SR for GAI prediction of winter oilseed rape, GAI_{SRuni} universal SR for GAI prediction, N_{SRww} crop-specific SR for N content prediction of winter wheat, N_{SRwosr} crop-specific SR for N content prediction of winter oilseed rape, N_{SRuni} universal SR for N content prediction, DM_{SRww} crop-specific SR for DM prediction of winter wheat, DM_{SRwosr} crop-specific SR for DM prediction of winter oilseed rape, DM_{SRuni} universal SR for DM prediction

Table 3 Mean absolute error (MAE) and the relative MAE (rMAE) of the established vegetation indices (VIs) for the estimation of green area index (GAI), total aboveground dry matter (DM), and total aboveground nitrogen content (N content) for the crops winter wheat (WW), winter oilseed rape (WOSR), winter barley (WB), and silage maize (SM) comprised in the Evaluation Set (Dataset I)

Crop parameter	VI	MAE (rMAE)			
		WW	WOSR	WB	SM
GAI	GAI_{SRww}	0.41 (15%)			
	GAI_{SRwosr}		0.25 (25%)		
	GAI_{SRuni}	0.42 (16%)	0.24 (24%)	0.35 (21%)	0.22 (20%)
N content [g m^{-2}]	N_{SRww}	1.62 (24%)			
	N_{SRwosr}		1.09 (43%)		
	N_{SRuni}	1.53 (22%)	1.76 (69%)	1.63 (34%)	2.43 (68%)
	N_{2step}	1.38 (32%)	0.68 (16%)	0.87 (20%)	0.93 (21%)
DM [g m^{-2}]	DM_{SRww}	50.41 (29%)			
	DM_{SRwosr}		52.23 (60%)		
	DM_{SRuni}	68.60 (39%)	55.61 (64%)	89.73 (57%)	45.98 (60%)
	DM_{2step}	50.46 (38%)	30.60 (23%)	91.81 (69%)	32.02 (24%)

GAI_{SRww} crop-specific SR for GAI prediction of winter wheat, GAI_{SRwosr} crop-specific SR for GAI prediction of winter oilseed rape, GAI_{SRuni} universal SR for GAI prediction, N_{SRww} crop-specific SR for N content prediction of winter wheat, N_{SRwosr} crop-specific SR for N content prediction of winter oilseed rape, N_{SRuni} universal SR for N content prediction, N_{2step} two-step model for N content prediction, DM_{SRww} crop-specific SR for DM prediction of winter wheat, DM_{SRwosr} crop-specific SR for DM prediction of winter oilseed rape, DM_{SRuni} universal SR for DM prediction, DM_{2step} two-step model for DM prediction

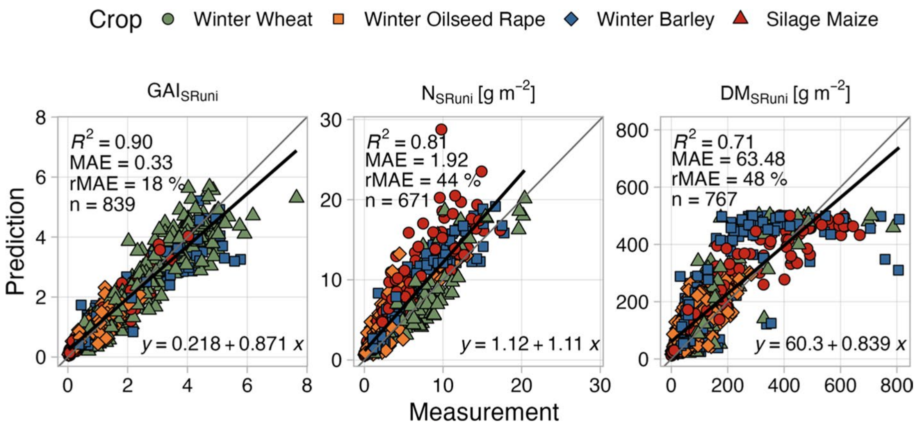

Fig. 2 Evaluation of the universal simple ratio vegetation indices for the estimation of green area index (GAI_{SRuni}), total aboveground N content (N_{SRuni}), and total aboveground dry matter (DM_{SRuni}). Equation, correlation coefficient (R^2), mean absolute error (MAE), relative MAE (rMAE), and number of observations (n) of the linear regression of measured vs. predicted values (different colors and shapes represent different crops of the Evaluation Set)

0.85 to 0.92 (Table 2). However, the evaluation revealed crop, year, and N treatment effects (Fig. 2; Table 4). This led to much higher MAEs (50.41–63.48 g m^2) and rMAEs (29–48%) regarding the evaluation (Fig. 2; Table 3).

Table 4 Adjusted correlation coefficient (R^2 adj.) and the fraction of additionally explained variance due to the factors crop (C), N treatment (N), harvest year (Y), and the combination of these (C x N x Y) of the established vegetation indices (VIs) for the estimation of green area index (GAI), total aboveground dry matter (DM), and total aboveground nitrogen content (N content) in the Evaluation Set (Dataset I)

Crop parameter	VI	R^2 adj.	Fraction of additional explained variance			
			C	N	Y	C x N x Y
GAI	GAI_{SRww}	0.858		0.028	0.022	0.032
	GAI_{SRwosr}	0.672		0.06	0.115	0.122
	GAI_{SRuni}	0.899	0.005	0.006	0.011	0.023
N content	N_{SRww}	0.829		0.05	0.077	0.117
	N_{SRwosr}	0.799		0.108	0.066	0.135
	N_{SRuni}	0.809	0.055	0.056	0.05	0.125
	N_{2step}	0.879	0.025	0.022	0.011	0.066
DM	DM_{SRww}	0.773		0.08	0.108	0.151
	DM_{SRwosr}	0.669		0.026	0.104	0.146
	DM_{SRuni}	0.708	0.024	0.037	0.084	0.177
	DM_{2step}	0.771	0.076	0.058	0.091	0.16

GAI_{SRww} crop-specific SR for GAI prediction of winter wheat, GAI_{SRwosr} crop-specific SR for GAI prediction of winter oilseed rape, GAI_{SRuni} universal SR for GAI prediction, N_{SRww} crop-specific SR for N content prediction of winter wheat, N_{SRwosr} crop-specific SR for N content prediction of winter oilseed rape, N_{SRuni} universal SR for N content prediction, N_{2step} two-step model for N content prediction, DM_{SRww} crop-specific SR for DM prediction of winter wheat, DM_{SRwosr} crop-specific SR for DM prediction of winter oilseed rape, DM_{SRuni} universal SR for DM prediction, DM_{2step} two-step model for DM prediction

Calibration and evaluation of functional two-step models for secondary crop parameters

The functional two-step models for the estimation of the secondary crop parameters DM (DM_{2step}) and N content (N_{2step}) based upon the assumption of a strong but crop-specific correlation between these secondary traits and the primary trait GAI. GAI was predicted by GAI_{SRuni} and multiplied with the species-, N treatment-, and period-specific correlations between the crop parameters detected in Dataset II (Fig. 3).

A power function characterized the relation of GAI and DM for all tested crops (Fig. 3). The correlations for winter wheat and winter barley of the plots without N fertilization differed from the plots with added N fertilization. For silage maize and winter oilseed rape, no impact of the N treatment occurred.

The power function approach was also used to depict the relation between GAI and N content for winter wheat and winter barley. In contrast, the crops silage maize and winter oilseed rape showed a linear correlation (Fig. 3). In silage maize, winter wheat, and winter barley the correlations of the plots without N fertilization differed from the plots with added N fertilization. In some crops, additionally, significant differences between higher N treatments occurred. However, the slopes of the equations varied only slightly. Thus, these differences were regarded to be not relevant for the application in the functional two-step N content model. Only winter oilseed rape did not react on N treatment. However, the relationship between GAI and N content was different depending on the sampling period (autumn and spring). For the fertilized plots and the data from spring samplings, respectively, a steeper slope was found.

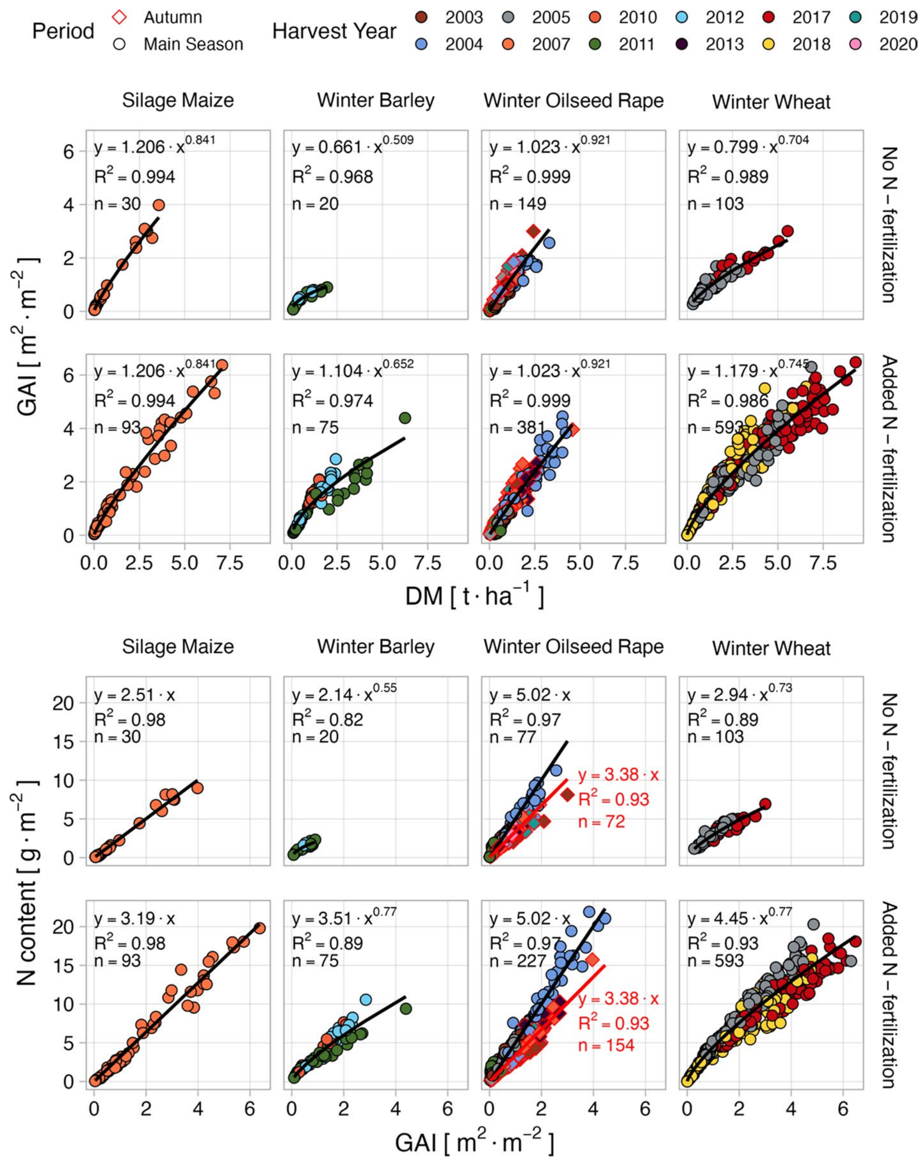

Fig. 3 Relationship of green area index (GAI) and total aboveground dry matter (DM) and relationship of GAI and total aboveground N content (N content) for the crops of Dataset II (silage maize, winter barley, winter oilseed rape and winter wheat) with no N-fertilization and added N-fertilization. Equation and correlation coefficient (R^2) of the relationship, and number of observations (n) (different fill colors represent different harvest years, different shapes and different border colors represent different sampling periods)

The close relations between the crop parameters existed until BBCH stage 39 (flag leave fully unrolled / 9 or more nodes detectable) for all tested crops excluding winter oilseed rape. Winter oilseed rape showed a stable correlation up to BBCH stage 59 (first petals visible, flower buds still closed). Afterwards the correlations between GAI, DM, and N content collapsed (data not shown).

The two-step approach for N content estimation (N_{2step}) had a R^2 of 0.88, a MAE of 0.95 g m^{-2}, and a rMAE of 22% (Fig. 4). N_{2step} was not improved by crop, year, and N treatment, or the combination of these as additional factors (Table 4). The N content was well predictable for all crops of the Evaluation Set by using this advanced two-step N model (Fig. 4).

The evaluation of DM_{2step} resulted in a R^2 of 0.77, a MAE of 49.92 g m^{-2}, and a rMAE of 37% and did not show saturation effects (Fig. 4). However, the model was biased by additional factors, particularly high by the factor harvest year (Table 4). For example, the accumulated DM of winter wheat and winter barley in 2018 was overestimated.

Development of an advanced functional model for DM prediction

An advanced functional model for DM prediction throughout the whole growing period was devised. The approach based upon a close crop-specific correlation between the accumulated DM and the intercepted radiation.

GAI_{SRuni} was applied to Dataset III, and a plausible GAI development through the whole growing season was estimated for each plot (data not shown). For each crop and at any point in time, the calculated radiation absorption showed a close correlation with the accumulated DM (Fig. 5). Nevertheless, the relation was affected by crop, harvest year, and N treatment. The RUEs for winter wheat, winter barley, and silage maize were 2.06, 2.23 and 2.22 g MJ^{-1}, respectively (Fig. 5).

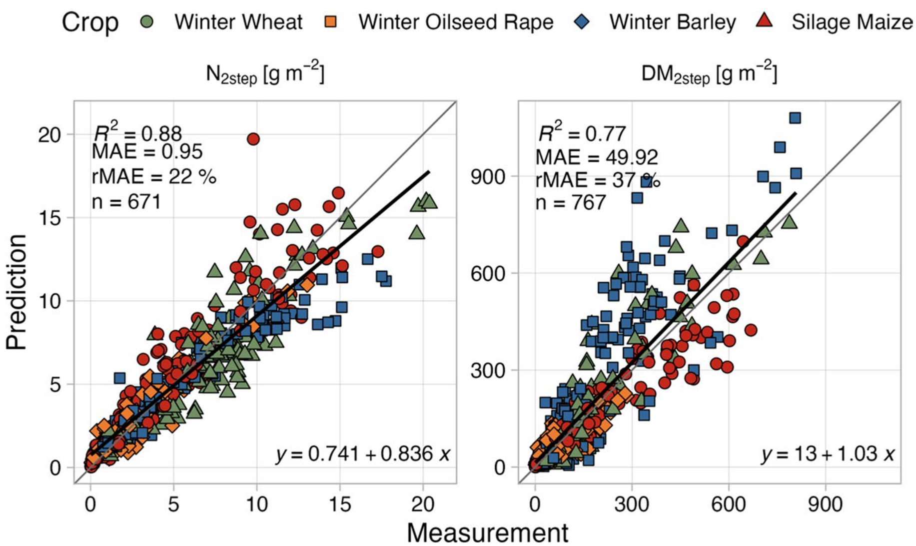

Fig. 4 Evaluation of the functional two-step models for the estimation of total aboveground N content (N_{2step}) and total aboveground dry matter (DM_{2step}). Equation, correlation coefficient (R^2), mean absolute error (MAE), relative MAE (rMAE), and number of observations (n) of the linear regression of measured vs. predicted values (different colors and shapes represent different crops of the Evaluation Set)

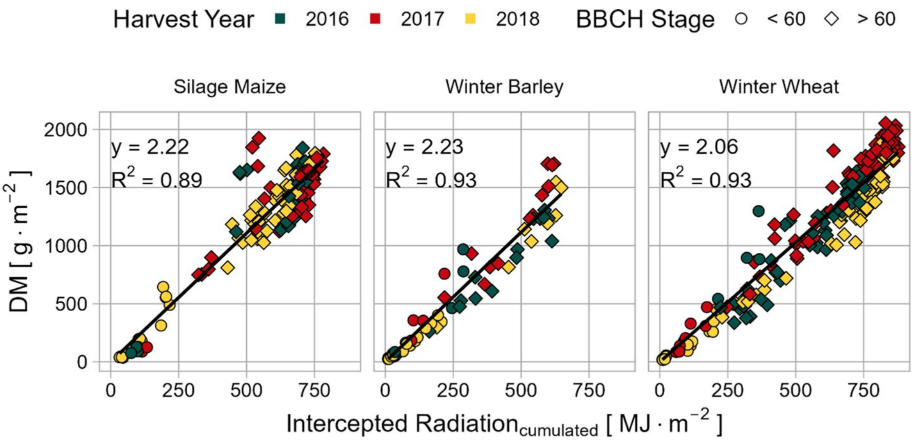

Fig. 5 Correlation of the cumulated intercepted radiation and the accumulated total aboveground dry matter (DM) for the crops of Dataset III (silage maize, winter barley, and winter wheat). Equation and correlation coefficient (R^2) of the relationship (different colors represent different harvest years, different shapes represent different developmental stages)

Discussion

Model calibration and evaluation of simple ratio vegetation indices for the target crop parameters

The best wavelength combination for the universal GAI model (GAI_{SRuni}) combined one wavelength of the near-infrared (NIR) and one of the red-edge (RE) region (Table 2). This was consistent with several other studies in which the RE region was found to be very important for the prediction of various crop parameters (e.g., Delegido et al., 2013; Gitelson et al., 2005; Kanning et al., 2018). But for convincing results the exact position of the wavelength in the rather small RE range is crucial (Kira et al., 2016; Thenkabail et al., 2000). However, this might cause problems when using data provided by multispectral remote sensing systems with restricted fixed wavebands, such as Sentinel-2 (Bukowiecki et al., 2021).

In general accordance with many studies (e.g., Bukowiecki et al., 2020; Duveiller et al., 2011; Haboudane et al., 2004; Kira et al., 2016; Müller et al., 2008; Nguy-Robertson et al., 2012), in the presented study crop-specific and universal SRs for GAI estimation were derived from the spectral reflectance measurements. The crop-specific SRs did not outclass the universal approach (GAI_{SRuni}) neither in the calibration nor in the evaluation (Tables 2, 3). Additionally, it should be stressed that GAI_{SRuni} was even able to predict reliable GAI values for crops which were not included in its calibration (Fig. 2). The high independence from crop and nitrogen fertilization (Table 4) was surprising, considering the strong effect of other canopy and leaf properties like leaf angle and chlorophyll concentration that are predicted by radiative transfer models (Berger et al., 2018). No influence of N fertilization and wheat cultivar have been observed before by Bukowiecki et al. (2020). This discrepancy between process understanding and empirical data seems to be insufficiently understood. Possibly, the effects of different optical leaf properties and canopy architectures are just moderate in comparison to other sources of variation. Nevertheless, on the base of the given process understanding all transfers of the empirical equations should be conducted with great care.

The quadratic fit of the universal GAI model and the slope of the evaluation (0.871) indicated that higher GAI values were slightly underestimated by GAI_{SRuni} (Table 2; Fig. 2). Many published models are only sensitive to a specific range of GAI values. This strongly limits their applicability because, for example, GAIs exceeding certain values are not predictable in a conceiving way (Bukowiecki et al., 2020; Delegido et al., 2013; Nguy-Robertson et al., 2014; Rosso et al., 2022; Serrano et al., 2000). However, Dataset I included a very wide range of GAI values (0–7.7, Table 1), and in the evaluation no obvious saturation was apparent (Fig. 2). Hence, GAI_{SRuni} was assumed to be well applicable at least for the crops and the GAI range considered in this study and the close relation between GAI and the spectral reflectance signal was confirmed.

The established universal SRs for the prediction of DM and N content were not robust, i.e., affected by harvest year, crop, and N treatment (Fig. 2; Table 4). However, also the evaluation of the crop-specific SRs showed scattering and saturation due to confounding factors resulting in sharply increased MAEs and rMAEs (Table 3). Saturating and varying (by harvest year, growing stage, and N treatment) relationships between VIs and these crop parameters have often been mentioned in literature (e.g., Basso et al., 2016; Hansen & Schjoerring, 2003; Müller et al., 2008; Serrano et al., 2000; Winterhalter et al., 2011). A close nearly linear relation between spectral reflectance and GAI is a well-known fact (e.g., Christensen & Goudriaan 1993; Tucker et al., 1981; Weiss et al., 2020) and was also apparent in Dataset I (Fig. 2; Tables 2, 3). Hence, the results concerning SRs for the prediction of N content and DM indicated that the relationship between these crop parameters and the spectral reflection was affected by further confounding factors. Strong correlations between DM, N content, and GAI during the vegetative growth period are accepted (e.g., Gabriel et al., 2017; Lemaire et al., 2008; Vos & van der Putten, 1998). However, GAI and DM as well as N content and DM are allometrically related (Lemaire et al., 2007; Ratjen et al., 2018). Presumably, the strong saturation effects determined for DM_{SRuni} (Fig. 2) were due to the non-linear relation between GAI and DM in contrast to the nearly linear relation between GAI and the spectral reflectance. Additionally, the relation between GAI and N content is crop-specific and depends on metabolic differences, the "leafiness coefficient", and the response patterns towards N deficiency. This results in a different DM accumulation or N content at the same GAI unit depending on the crop species and the N availability (Lemaire et al., 2008; Ratjen et al., 2018). Obviously, such differences were not depictable by the established SRs. This was supported by the fact that Dataset I (except of winter oilseed rape) had to be restricted to samples collected before the end of BBCH main stage 3 (stem elongation). Afterwards, N and the accumulated DM are stored in parts of the plants that are no longer green (Christensen & Goudriaan, 1993).

All in all, these results supported the classification of crop parameters in primary and secondary traits as proposed by Weiss et al. (2020). Additionally, the first working hypothesis was partly confirmed: GAI can be assumed as the primary determinant of the spectral reflectance. Hence, VIs for the estimation of this crop parameter can be calibrated universally over a wide range of different crop species. In contrast, secondary traits, such as N content and DM, are not directly derivable from spectral reflectance measurements because they depend on underlying factors which do not directly affect spectral reflectance signal.

Calibration and evaluation of functional two-step models for secondary crop parameters

Functional two-step models were proposed for the prediction of the secondary crop parameters DM (DM_{2step}) and N content (N_{2step}). The approach based on the disentanglement of the primary and the secondary traits and existing fundamental relationships between these crop parameters (Lemaire et al., 2019). Close crop-specific correlations between GAI and DM or GAI and N content, respectively, were confirmed in Dataset II supporting findings from other authors (e.g., Lemaire et al., 2008; Massignam et al., 2011; Plénet & Lemaire, 2000). For winter wheat, scattering occurred which was partly explained by the weather conditions in the different years, primary the precipitation during the main growing period in April and May. Since the only response of winter oilseed rape to N limitation was a GAI reduction, this crop might be a good predictor for soil N supply. In accordance with Lemaire et al. (2007), all tested relationships were restricted to the vegetative growth period (Fig. 3). This is because afterwards the accumulated DM and N were stored in parts of the plants which are no longer green resulting in a collapse of the correlations.

The estimation of the N content was considerably improved by the application of N_{2step} (Table 3). However, it is vitally important that detected response patterns between N content and GAI are only applicable for the specific conditions under which the data were collected (Lemaire et al., 2019). Consequently, Fu et al. (2021) stated that data-driven models for crop N status prediction must be handled with extreme care because the calibration is only valid for datasets with the same or at least similar conditions (e.g., environment, water status, crop species). However, the underlying datasets comprised various growing seasons. Thereby, different weather conditions were depicted. Additionally, the proposed N_{2step} approach seems to be generally promising for the application in site-specific N management strategies. Because GAI was shown to be predictable quite robustly, only knowledge about the specific correlation between N content and GAI is needed. Due to various works, such data are already available for many environments and crops.

Compared to the universal and crop-specific SRs for DM estimation, the application of DM_{2step} mostly resulted in better evaluation results (Table 3). However, following Lemaire et al. (2008) the crop-specific relation between GAI and accumulated DM is strongly affected by environmental conditions. For example, such effects were reflected in the overestimation of DM of winter wheat and winter barley in 2018 because this vegetation period was particularly dry at the experimental side resulting in different relationships between GAI and DM.

In general, the disentanglement of secondary and primary traits by the consideration of fundamental relationships provided more robust prediction models as stated in the second working hypothesis. However, especially the DM prediction was still affected by confounding variables which were not depictable by DM_{2step}. Additionally, both established functional two-step models were only valid for the vegetative growth period. In context of crop N status estimation, this is no disadvantage since N fertilization takes place during this period. However, the prediction of DM accumulation is mainly of interest for final yield prediction, thus, the limitation to the vegetative growth period of DM_{2step} is problematic.

Development of an advanced functional model for DM prediction

The applicability of many VIs in agricultural research and precision agriculture is strongly limited since the large majority of VIs was calibrated for a specific crop and a certain period (e.g., Aase & Siddoway, 1981; Hansen & Schjoerring, 2003; Müller et al., 2008; Rosso et al., 2022). This also applied to the established models in the presented study since Dataset I and Dataset II were restricted to measurements within the vegetative growth period. However, an accurate DM estimation is important for the final yield prediction. Thus, a whole-season model for DM prediction would be desirable.

The proposed advanced functional DM model based on a close relation between accumulated DM and the amount of intercepted radiation at any given point during the growing season (Monteith, 1977). To calculate the intercepted radiation, a GAI model that was valid for the whole growing season was necessary. However, GAI_{SRuni} was only evaluated for the vegetative growth period. The destructive determination of GAI during ripening and senescence is nearly impossible and very error-prone due to the inhomogeneous senescence of the plant material and the gradual degradation of leaf chlorophyll (Bukowiecki et al., 2020). Thus, a simple expansion of the Evaluation Set to the generative growth period was not possible. It has been reported that the predictive quality of various GAI models significantly decreased during ripening and senescence (e.g., Boegh et al., 2002; Dong et al., 2020; Duveiller et al., 2011; Haboudane et al., 2004; Richter et al., 2012). However, Bukowiecki et al. (2020) showed that different GAI models for winter wheat, which were calibrated without any senescence data, were able to predict reliable GAI values throughout the whole growing season. Bukowiecki et al. (2020) traced the decreasing performance of GAI models mentioned by other authors back to problems in the sampling of the ground truth data rather than to a missing correlation between the spectral reflectance signal and GAI within the senescence phase.

These hypotheses were implicitly confirmed by the strong correlation between the intercepted radiation, which was calculated from predicted GAI values, and the accumulated DM at any point in time, including senescence and final harvest (Fig. 5). These relationships were crop specific and its slopes represented the RUE. The resulting RUEs (Fig. 5) were in accordance with values mentioned by other authors (e.g., Fletcher et al., 2013; Jamieson et al., 1995; Lindquist et al., 2005; Rose et al., 2017; Sieling et al., 2016). With knowledge of the specific RUE and periodic spectral reflectance measurements (to derive GAI values), quite accurate predictions of the accumulated DM throughout the whole growing period are possible. However, it must be pointed out that the RUE depends on various additional factors, such as crop species, environmental conditions, and N availability (Ciampitti et al., 2013; Gabriel et al., 2017; Ratjen & Kage, 2016). This fact limits the applicability of this approach for DM estimation and might be attenuated by the assimilation of the GAI values into crop growth models. Moreover, for final yield prediction, lacking information about the harvest index may be seen as a limiting factor. The harvest index is influenced by many variables like cultivar, management, and year (Rose & Kage, 2019). Additionally, the harvest index is not detectable through spectral reflectance data. Nevertheless, this advanced functional model approach seems to be more promising than a simple empirical estimation of grain yield from single in-season spectral reflection measurements.

Conclusion

The analyzes of the large dataset add evidence that spectral reflectance data (400–900 nm) exclusively reveal information about the green parts of a crop. Hence, GAI is the main driver of the reflectance signal allowing the calibration of a rather robust and easy-to-handle SR for the prediction of GAI that was applicable throughout the whole growing season without a crop-specific parametrization. Nevertheless, the universality of the SR is limited and should be tested in further datasets containing additional crops and experimental sites. Other crop parameters are mainly indirectly derived from reflectance measurements in the visible and NIR range. However, these two implicit independent processes were made explicit by two-step and advanced functional models which considered fundamental relationships between the crop parameters. This disentanglement allowed to combine non-orthogonal datasets, enhanced the selection of functional representation, facilitated the detection of confounding variables, and widened the usefulness of the established universal (without crop-specific parametrization) GAI model. The relationships between secondary and primary crop parameters are influenced by a multitude of factors and the range of applicability of empirical equations need to be handled with care.

Acknowledgements This study benefits from various projects conducted in the last two decades. The authors thank all persons who contributed to the development of the large dataset.

Authors contributions Conceptualization: MR, TR, HK; Methodology: MR, TR, HK; Data curation: MR; Formal analysis: MR, TR; Investigation: MR; Writing—original draft preparation: MR; Writing—review and editing: TR, HK; Supervision: HK.

Funding Open Access funding enabled and organized by Projekt DEAL.

Data availability The datasets generated during and/or analyzed during the current study are available from the corresponding author on reasonable request.

Declarations

Conflict of interest The authors declare that they have no conflict of interest.

References

Aase, J. K., & Siddoway, F. H. (1981). Assessing winter wheat dry matter production via spectral reflectance measurements. *Remote Sensing of Environment*, *11*, 267–277. https://doi.org/10.1016/0034-4257(81)90025-0

Basso, B., Fiorentino, C., Cammarano, D., & Schulthess, U. (2016). Variable rate nitrogen fertilizer response in wheat using remote sensing. *Precision Agriculture*, *17*(2), 168–182. https://doi.org/10.1007/s11119-015-9414-9

Berger, K., Atzberger, C., Danner, M., D'Urso, G., Mauser, W., Vuolo, F., & Hank, T. (2018). Evaluation of the PROSAIL model capabilities for future hyperspectral model environments: A review study. In *Remote Sensing* (Vol. 10, Issue 1). MDPI AG. https://doi.org/10.3390/rs10010085

Boegh, E., Soegaard, H., Broge, N., Hasager, C. B., Jensen, N. O., Schelde, K., & Thomsen, A. (2002). Airborne multispectral data for quantifying leaf area index, nitrogen concentration, and photosynthetic efficiency in agriculture. *Remote Sensing of Environment*, *81*(2–3), 179–193. https://doi.org/10.1016/S0034-4257(01)00342-X

Bukowiecki, J., Rose, T., Ehlers, R., & Kage, H. (2020). High-throughput prediction of whole season green area index in winter wheat with an airborne multispectral sensor. *Frontiers in Plant Science*. https://doi.org/10.3389/fpls.2019.01798

Bukowiecki, J., Rose, T., & Kage, H. (2021). Sentinel-2 data for precision agriculture?—A UAV-based assessment. *Sensors (Basel, Switzerland)*, *21*(8), https://doi.org/10.3390/s21082861

Christensen, S., & Goudriaan, J. (1993). Deriving light interception and biomass from spectral reflectance ratio. *Remote Sensing of Environment*, *43*(1), 87–95. https://doi.org/10.1016/0034-4257(93)90066-7

Ciampitti, I. A., Murrell, S. T., Camberato, J. J., Tuinstra, M., Xia, Y., Friedemann, P., & Vyn, T. J. (2013). Physiological dynamics of maize nitrogen uptake and partitioning in response to plant density and N stress factors: I. Vegetative phase. *Crop Science*, *53*(5), 2105–2119. https://doi.org/10.2135/cropsci2013.01.0040

Claverie, M., Demarez, V., Duchemin, B., Hagolle, O., Ducrot, D., Marais-Sicre, C., Dejoux, J. F., Huc, M., Keravec, P., Béziat, P., Fieuzal, R., Ceschia, E., & Dedieu, G. (2012). Maize and sunflower biomass estimation in southwest France using high spatial and temporal resolution remote sensing data. *Remote Sensing of Environment*, *124*, 844–857. https://doi.org/10.1016/j.rse.2012.04.005

Clevers, J. G. P. W., & Gitelson, A. A. (2013). Remote estimation of crop and grass chlorophyll and nitrogen content using red-edge bands on sentinel-2 and-3. *International Journal of Applied Earth Observation and Geoinformation*, *23*(1), 344–351. https://doi.org/10.1016/j.jag.2012.10.008

Clevers, J. G. P. W., & Kooistra, L. (2012). Using hyperspectral remote sensing data for retrieving canopy chlorophyll and nitrogen content. *IEEE Journal of Selected Topics in Applied Earth Observations and Remote Sensing*, *5*(2), 574–583. https://doi.org/10.1109/JSTARS.2011.2176468

Delegido, J., Verrelst, J., Meza, C. M., Rivera, J. P., Alonso, L., & Moreno, J. (2013). A red-edge spectral index for remote sensing estimation of green LAI over agroecosystems. *European Journal of Agronomy*, *46*, 42–52. https://doi.org/10.1016/j.eja.2012.12.001

Demetriades-Shah, T. H., Steven, M. D., & Clark, J. A. (1990). High resolution derivative spectra in remote sensing. *Remote Sensing of Environment*, *33*(1), 55–64. https://doi.org/10.1016/0034-4257(90)90055-Q

Dong, T., Liu, J., Qian, B., He, L., Liu, J., Wang, R., Jing, Q., Champagne, C., McNairn, H., Powers, J., Shi, Y., Chen, J. M., & Shang, J. (2020). Estimating crop biomass using leaf area index derived from Landsat 8 and Sentinel-2 data. *ISPRS Journal of Photogrammetry and Remote Sensing*, *168*, 236–250. https://doi.org/10.1016/j.isprsjprs.2020.08.003

Duveiller, G., Weiss, M., Baret, F., & Defourny, P. (2011). Retrieving wheat Green Area Index during the growing season from optical time series measurements based on neural network radiative transfer inversion. *Remote Sensing of Environment*, *115*(3), 887–896. https://doi.org/10.1016/j.rse.2010.11.016

Fletcher, A. L., Johnstone, P. R., Chakwizira, E., & Brown, H. E. (2013). Radiation capture and radiation use efficiency in response to N supply for crop species with contrasting canopies. *Field Crops Research*, *150*, 126–134. https://doi.org/10.1016/j.fcr.2013.06.014

Food and Agriculture Organization of the United Nations. (2014). *World reference base for soil resources 2014: international soil classification system for naming soils and creating legends for soil maps (Update 2015)*. FAO

Fu, Y., Yang, G., Pu, R., Li, Z., Li, H., Xu, X., Song, X., Yang, X., & Zhao, C. (2021). An overview of crop nitrogen status assessment using hyperspectral remote sensing: Current status and perspectives. *European Journal of Agronomy*, *Vol. 124*, https://doi.org/10.1016/j.eja.2021.126241. Elsevier B.V

Gabriel, J. L., Zarco-Tejada, P. J., López-Herrera, P. J., Pérez-Martín, E., Alonso-Ayuso, M., & Quemada, M. (2017). Airborne and ground level sensors for monitoring nitrogen status in a maize crop. *Biosystems Engineering*, *160*, 124–133. https://doi.org/10.1016/j.biosystemseng.2017.06.003

Gerighausen, H., Lilienthal, H., Jarmer, T., & Siegmann, B. (2015). Evaluation of leaf area index and dry matter predictions for crop growth modelLing and yield estimation based on field reflectance measurements. *EARSeL EProceedings*, *14*(2), 71–90. https://doi.org/10.12760/02-2015-2-06

Gitelson, A. A., Gritz, Y., & Merzlyak, M. N. (2003). Relationships between leaf chlorophyll content and spectral reflectance and algorithms for non-destructive chlorophyll assessment in higher plant leaves. *Journal Of Plant Physiology*, *160*(3), 271–282. https://doi.org/10.1078/0176-1617-00887

Gitelson, A. A., Viña, A., Ciganda, V., Rundquist, D. C., & Arkebauer, T. J. (2005). Remote estimation of canopy chlorophyll content in crops. *Geophysical Research Letters*, *32*(8), 1–4. https://doi.org/10.1029/2005GL022688

Haboudane, D., Miller, J. R., Pattey, E., Zarco-Tejada, P. J., & Strachan, I. B. (2004). Hyperspectral vegetation indices and novel algorithms for predicting green LAI of crop canopies: Modeling and validation in the context of precision agriculture. *Remote Sensing of Environment*, *90*(3), 337–352. https://doi.org/10.1016/j.rse.2003.12.013

Hansen, P. M., & Schjoerring, J. K. (2003). Reflectance measurement of canopy biomass and nitrogen status in wheat crops using normalized difference vegetation indices and partial least squares regression. *Remote Sensing of Environment*, *86*(4), 542–553. https://doi.org/10.1016/S0034-4257(03)00131-7

Jamieson, P. D., Martin, R. J., Francis, G. S., & Wilson, D. R. (1995). Drought effects on biomass production and radiation-use efficiency in barley. *Field Crops Research*, *43*(2–3), 77–86. https://doi.org/10.1016/0378-4290(95)00042-O

Jordan, C. F. (1969). Derivation of Leaf-Area Index from quality of light on the forest floor. *Ecology*, *50*(4), 663–666. https://doi.org/10.2307/1936256

Kanning, M., Kühling, I., Trautz, D., & Jarmer, T. (2018). High-resolution UAV-based hyperspectral imagery for LAI and chlorophyll estimations from wheat for yield prediction. *Remote Sensing*, *10*(12), https://doi.org/10.3390/rs10122000

Kira, O., Nguy-Robertson, A. L., Arkebauer, T. J., Linker, R., & Gitelson, A. A. (2016). Informative spectral bands for remote green LAI estimation in C3 and C4 crops. *Agricultural and Forest Meteorology*, *218–219*, 243–249. https://doi.org/10.1016/j.agrformet.2015.12.064

Lemaire, G., Sinclair, T., Sadras, V., & Bélanger, G. (2019). Allometric approach to crop nutrition and implications for crop diagnosis and phenotyping. A review. *Agronomy for Sustainable Development*, *39*(2), 1–17. https://doi.org/10.1007/s13593-019-0570-6

Lemaire, G., Tang, L., Bélanger, G., Zhu, Y., & Jeuffroy, M. H. (2021). Forward new paradigms for crop mineral nutrition and fertilization towards sustainable agriculture. *European Journal of Agronomy*, *125*. https://doi.org/10.1016/j.eja.2021.126248

Lemaire, G., van Oosterom, E., Jeuffroy, M. H., Gastal, F., & Massignam, A. (2008). Crop species present different qualitative types of response to N deficiency during their vegetative growth. *Field Crops Research*, *105*(3), 253–265. https://doi.org/10.1016/j.fcr.2007.10.009

Lemaire, G., van Oosterom, E., Sheehy, J., Jeuffroy, M. H., Massignam, A., & Rossato, L. (2007). Is crop N demand more closely related to dry matter accumulation or leaf area expansion during vegetative growth? *Field Crops Research*, *100*(1), 91–106. https://doi.org/10.1016/j.fcr.2006.05.009

Lindquist, J. L., Arkebauer, T. J., Walters, D. T., Cassman, K. G., & Dobermann, A. (2005). Maize radiation use efficiency under optimal growth conditions. *Agronomy Journal*, *97*(1), 72–78. https://doi.org/10.2134/agronj2005.0072

Ma, Y., Fang, S., Peng, Y., Gong, Y., & Wang, D. (2019). Remote estimation of biomass in winter oilseed rape (*Brassica napus* L.) using canopy hyperspectral data at different growth stages. *Applied Sciences (Switzerland)*, *9*(3), https://doi.org/10.3390/app9030545

Massignam, A. M., Chapman, S. C., Hammer, G. L., & Fukai, S. (2011). Effects of nitrogen supply on canopy development of maize and sunflower. *Crop and Pasture Science*, *62*(12), 1045–1055. https://doi.org/10.1071/CP11165

Meier, U. (1997). *Growth stages of mono- and dicotyledonous plants*. Blackwell Wissenschafts-Verlag

Monsi, M., & Saeki, T. (1953). The light factor in plant communities and its significance for dry matter production. *Japanese Journal of Botany*, *14*(1), 22–52

Monteith, J. L. (1977). Climate and the efficiency of crop production in Britain. *Philosophical Transactions of the Royal Society of London B: Biological Sciences*, *281*(980), 277–294. https://doi.org/10.1098/rstb.1977.0140

Muchow, R. C., & Sinclair, T. R. (1994). Nitrogen response of leaf photosynthesis and canopy radiation use efficiency in field-grown maize and sorghum. *Crop Science*, *34*(3), 721–727. https://doi.org/10.2135/cropsci1994.0011183X003400030022x

Müller, K., Böttcher, U., Meyer-Schatz, F., & Kage, H. (2008). Analysis of vegetation indices derived from hyperspectral reflection measurements for estimating crop canopy parameters of oilseed rape (*Brassica napus* L.). *Biosystems Engineering*, *101*(2), 172–182. https://doi.org/10.1016/j.biosystemseng.2008.07.004

Nguy-Robertson, A., Gitelson, A., Peng, Y., Viña, A., Arkebauer, T., & Rundquist, D. (2012). Green leaf area index estimation in maize and soybean: Combining vegetation indices to achieve maximal sensitivity. *Agronomy Journal*, *104*(5), 1336–1347. https://doi.org/10.2134/agronj2012.0065

Nguy-Robertson, A., Peng, Y., Gitelson, A. A., Arkebauer, T. J., Pimstein, A., Herrmann, I., Karnieli, A., Rundquist, D. C., & Bonfil, D. J. (2014). Estimating green LAI in four crops: Potential of determining optimal spectral bands for a universal algorithm. *Agricultural and Forest Meteorology*, *192–193*, 140–148. https://doi.org/10.1016/j.agrformet.2014.03.004

Plénet, D., & Lemaire, G. (2000). Relationships between dynamics of nitrogen uptake and dry matter accumulation in maize crops. Determination of critical N concentration. *Plant and Soil*, *216*, 65–82. https://doi.org/10.1023/A:1004783431055

R Core Team (2000). *R: A language and environment for statistical computing*

Ratjen, A. M., & Kage, H. (2016). Nitrogen-limited light use efficiency in wheat crop simulators: Comparing three model approaches. *Journal of Agricultural Science*, *154*(6), 1090–1101. https://doi.org/10.1017/S0021859615001082

Ratjen, A. M., Lemaire, G., Kage, H., Plénet, D., & Justes, E. (2018). Key variables for simulating leaf area and N status: Biomass based relations versus phenology driven approaches. *European Journal of Agronomy*, *100*, 110–117. https://doi.org/10.1016/j.eja.2018.04.008

Richter, K., Hank, T. B., Vuolo, F., Mauser, W., & D'Urso, G. (2012). Optimal exploitation of the sentinel-2 spectral capabilities for crop leaf area index mapping. *Remote Sensing*, *4*(3), 561–582. https://doi.org/10.3390/rs4030561

Rose, T., & Kage, H. (2019). The contribution of functional traits to the breeding progress of Central-European winter wheat under differing crop management intensities. *Frontiers in Plant Science*. https://doi.org/10.3389/fpls.2019.01521

Rose, T., Nagler, S., & Kage, H. (2017). Yield formation of Central-European winter wheat cultivars on a large scale perspective. *European Journal of Agronomy*, *86*, 93–102. https://doi.org/10.1016/j.eja.2017.03.003

Rosso, P., Nendel, C., Gilardi, N., Udroiu, C., & Chlebowski, F. (2022). Processing of remote sensing information to retrieve leaf area index in barley: A comparison of methods. *Precision Agriculture*. https://doi.org/10.1007/s11119-022-09893-4

Serrano, L., Filella, I., & Peñuelas, J. (2000). Remote sensing of biomass and yield of winter wheat under different nitrogen supplies. *Crop Science*, *40*(3), 723–731. https://doi.org/10.2135/cropsci2000.403723x

Sieling, K., Böttcher, U., & Kage, H. (2016). Dry matter partitioning and canopy traits in wheat and barley under varying N supply. *European Journal of Agronomy*, *74*, 1–8. https://doi.org/10.1016/j.eja.2015.11.022

Thenkabail, P. S., Smith, R. B., & de Pauw, E. (2000). Hyperspectral vegetation indices and their relationships with agricultural crop characteristics. *Remote Sensing of Environment*, *71*(2), 158–182. https://doi.org/10.1016/S0034-4257(99)00067-X

Tucker, C. J., Holben, B. N., Elgin, J. H., & McMURTREY, J. E. III (1981). Remote sensing of total dry-matter accumulation in winter wheat. *Remote Sensing of Environment*, *11*, 171–189. https://doi.org/10.1016/0034-4257(81)90018-3

Viña, A., Gitelson, A. A., Nguy-Robertson, A. L., & Peng, Y. (2011). Comparison of different vegetation indices for the remote assessment of green leaf area index of crops. *Remote Sensing of Environment*, *115*(12), 3468–3478. https://doi.org/10.1016/j.rse.2011.08.010

Vos, J., & van der Putten, P. E. L. (1998). Effect of nitrogen supply on leaf growth, leaf nitrogen economy and photosynthetic capacity in potato. *Field Crops Research*, *59*(1), 63–72. https://doi.org/10.1016/S0378-4290(98)00107-5

Vos, J., van der Putten, P. E. L., & Birch, C. J. (2005). Effect of nitrogen supply on leaf appearance, leaf growth, leaf nitrogen economy and photosynthetic capacity in maize (*Zea mays* L.). *Field Crops Research*, *93*(1), 64–73. https://doi.org/10.1016/j.fcr.2004.09.013

Weiss, M., Jacob, F., & Duveiller, G. (2020). Remote sensing for agricultural applications: A meta-review. *Remote Sensing of Environment*, *236*. https://doi.org/10.1016/j.rse.2019.111402

Wickham, H. (2016). *ggplot2: Elegant graphics for data analysis*. Springer. https://doi.org/10.1007/978-3-319-24277-4_9

Winterhalter, L., Mistele, B., Jampatong, S., & Schmidhalter, U. (2011). High-throughput sensing of aerial biomass and above-ground nitrogen uptake in the vegetative stage of well-watered and drought stressed tropical maize hybrids. *Crop Science*, *51*(2), 479–489. https://doi.org/10.2135/cropsci2010.07.0397